Contrasting recent trends in Southern Hemisphere Westerlies across different ocean basins

Darryn W. Waugh[1,2*], Antara Banerjee[3,4], John C. Fyfe[5], Lorenzo M. Polvani[6]

[1]*Department of Earth and Planetary Sciences, Johns Hopkins University, Baltimore, MD*

[2]*School of Mathematics and Statistics, University of New South Wales, Sydney, New South Wales, Australia*

[3]*Cooperative Institute for Research in Environmental Sciences, University of Colorado Boulder, Boulder, CO, USA.*

[4]*Chemical Sciences Laboratory, National Oceanic and Atmospheric Administration, Boulder, CO, USA.*

[5]*Canadian Centre for Climate Modelling and Analysis, Environment and Climate Change Canada, Victoria, British Columbia, Canada.*

[6]*Department of Applied Physics and Applied Mathematics, Columbia University, New York, NY, USA.*

Corresponding author: Darryn Waugh (waugh@jhu.edu)

Key Points:

- There are substantial zonal variations in past trends in the magnitude and latitude of the peak Southern Hemisphere zonal winds
- The peak annual-mean zonal winds have moved equatorward over the Pacific but poleward over the Atlantic and Indian Oceans.
- Climate model simulations indicate that the differential movement of the westerlies is due to internal atmospheric variability.

Abstract

Many studies have documented the trends in the latitudinal position and strength of the midlatitude westerly jet in the Southern Hemisphere. However, very little attention has been paid to the longitudinal variations of these trends. Here, we specifically focus on the zonal asymmetries in the southern jet trends between 1980-2018. Meteorological reanalyses show a robust strengthening and an equatorward shift of the annual-mean and springtime jet over the Pacific sector, in contrast to a weaker strengthening and poleward shift over the Atlantic and Indian Ocean sectors. The reanalysis trends fall within the ensemble spread for historical climate model simulations, showing that climate models are able to capture the observed trends. Climate model simulations indicate that the differential movement of the jet is a manifestation of internal variability and is not a forced response. Implications of these asymmetries for other components of the climate system are discussed.

Plain Language Summary

The band of strong westerly winds in middle latitudes, which are often referred to as the midlatitude jet streams, influence not only temperature, regional storms, and precipitation but also the ocean circulation and amount of carbon and heat entering the oceans. In recent years, much attention has been paid to the observed strengthening and poleward shift of the Southern Hemisphere jet stream. However, nearly all the focus has rested on trends in longitudinally-averaged winds. Here we specifically focus on the longitudinal variations in the jet trends over the last four decades. Observationally-based data show a robust strengthening and an equatorward shift of the annual-mean jet over the Pacific Ocean, in contrast to a weaker strengthening and poleward shift over the Atlantic and Indian Oceans. Simulations with climate models indicate that the underlying cause of this differential movement of the jet is internal atmospheric variability, and not a response to human activities. The longitudinal variations in the jet trends may have consequences for ocean gyre circulations, and associated transport of heat and carbon into the oceans.

1 Introduction

The near-surface westerlies are a dominant feature of the midlatitude atmospheric circulation of the Southern Hemisphere (SH), influencing temperature, regional storms, and precipitation (e.g. Thompson and Wallace 2002, Hendon et al. 2007). In addition, these winds play a major role in driving the ocean circulation, and the uptake of carbon and heat (e.g., Hall and Visbeck 2002, Sen Gupta and England 2006, Toggweiler and Russell 2008). In recent years, much attention has been paid to an intensification and poleward shift of these westerlies over the last four decades (e.g., Thompson et al. 2011, Swart and Fyfe 2012, Swart et al. 2105), and the wider impacts on the atmosphere and oceans (e.g. Roemmich et al. 2007, Le Quere et al. 2007, Waugh et al. 2013). However, this attention has focused primarily on changes in the zonal-mean winds, and longitudinal variations have been largely overlooked. While changes in the mean meridional circulation (of the atmosphere and oceans) will likely be closely related to changes in the zonal-mean winds, the response of many other aspects, such as the subtropical gyre circulation and associated changes in ventilation, heat uptake, and sea level, will depend more on regional changes (e.g., Cai et al. 2010, Zhang et al. 2014, Jones et al. 2019, Waugh et al. 2019). It is therefore important to know whether regionally averaged winds have also intensified and moved poleward. Furthermore, most of the previous analysis of SH wind trends has been on the summer changes, when zonal-mean trends are the largest. However, the trends in annual-mean winds are likely the most relevant for ocean impacts, as the ocean response to changes in SH winds occurs over decadal or longer time scales.

In this study, we examine the zonal asymmetries in wind trends over the last four decades, and ask whether there has been a uniform strengthening and latitudinal shift in peak winds across the different ocean basins. This extends earlier studies by Schneider et al. (2015) and Swart et al (2015) who showed that there are spatial variations in past trends in near-surface winds, but did not examine the impact of these trends on the strength and position of the peak winds averaged over each ocean basin. Yang et al (2020) have very recently have examined zonal variations in jet trends, but they only considered summer trends. We show here that the winter-spring (and annual-mean) trends differ substantially from the summer trends.

We use near-surface winds from multiple meteorological reanalyses to quantify the changes since 1980, and examine the causes of these changes using multi-model ensembles from the Coupled Model Intercomparison Project phase 5 (CMIP5, Taylor et al., 2012) and large initial-condition ensembles from the Canadian Earth System Model version 2 (CanESM2, Gagné et al. 2017). These model ensembles have been previously used to examine trends and variability in the zonal-mean atmospheric circulation (e.g., Grise et al. 2019, Banerjee et al. 2020), and we extend these studies to consider zonal variations in trends. In combination, these ensembles enable comparison with observations as well as examination of the role atmosphere-ocean coupling and of different anthropogenic forcings.

2. Methods

We examine recent changes in the SH winds using three atmospheric reanalysis products: ERA-I (Dee etal 2011), JRA-55 (Kobayashi et al. 2015), and MERRA2 (Gelaro et al. 2017). We select these relatively recent reanalyses as older generation reanalyses have been shown to yield spurious trends and poorer agreement than newer reanalyses for metrics of the mid-latitude jet (e.g., Swart et al. 2015, Grise et al. 2019). We focus on the period from 1980 to 2018 which is common to all these reanalyses.

Two different types of model ensembles are used to ascertain the causes of the trends seen in the reanalyses. The first type are multi-model ensembles using climate models that participated in CMIP5. The ensembles examined include (i) "historical" simulations driven by all-known natural and anthropogenic forcings covering the period 1850–2005, (ii) atmosphere-only "AMIP" simulations driven by all forcings between 1979-2005 but with observed sea-surface temperatures (SSTs) and sea ice concentrations, (iii) preindustrial control (piControl) simulations at constant 1850 forcings, and (iv) "4xCO2" simulations with an instantaneous quadrupling of atmospheric CO_2 from piControl conditions. For each we model and scenario we analyze only the first ensemble member ("r1i1p1"), in order to weigh all models equally. We use these ensembles to make the following comparisons. Trends in the historical simulations are directly compared with observed trends. Comparison of the historical and AMIP simulations isolates the role of ocean-atmosphere coupling. Lastly, comparison of the 4xCO2 and piControl simulations isolates the forced response to a large increase in CO_2. We use monthly mean model output from 20 models, for which we have all simulations (see Supplementary Table 1); this is a subset of the 23 models considered in several earlier studies of changes in zonal-mean winds, e.g., Grise and Polvani (2014, 2016) and Waugh et al. (2018). We analyze trends over the 1980-2005 period for the CMIP5 historical and AMIP simulations, which end in 2005. For the response to 4xCO2, we average of the last 50 years of the 4xCO2 simulation and take the difference from the piControl climatology.

The second type of ensembles are large (50-member) initial-condition ensembles of simulations from a single model, CanESM2. For this there is a historical all-forcing ensemble (using the same forcing as the CMIP5 historical simulations) as well as three single-forcing ensembles where the only time varying forcing is (1) stratospheric ozone ("OZ"), (2) anthropogenic aerosols ("AA"), or (3) natural, volcanic and solar, ("NAT") forcings. Comparison of the CanESM2 ensembles allows us to isolate the role of different external forcings. As with the CMIP5 ensembles, we analyze the 1979-2005 period.

In both reanalyses and model output we examine the zonal wind fields at 850 hPa. Results are presented here for both zonal-mean winds, and for averages across the Pacific Ocean (150°E to 290°E) and the combined Atlantic-Indian Ocean (40°W to 120°E) sectors. Averages over the individual Atlantic and Indian produce similar results to the combined average, so we focus on the combined average for simplicity. We refer to the winds averaged over the Pacific Ocean as "the Pacific jet", and similarly winds averaged over the combined Atlantic-Indian Oceans as "the Atlantic-Indian jet". For all longitudinal averages, the jet latitude is defined as the latitude at which the zonal wind maximum occurs, and is found in the gridded data by analytically fitting a quadratic between the latitude of the largest value and 10° either side.

The statistical significance of the reanalysis trends is determined using the Student's t test with t statistic given by the estimated trend divided by the standard deviation. Following Swart et al. (2015), the uncertainty in the model ensemble mean trend (i.e. the forced trend) is represented by the (95%) confidence interval, which is given by $c\sigma/\sqrt{n}$, where n is number of models or members, σ^2 is the variance in trends across the ensemble members, and c is the 97.5th percentile of the Student's t distribution with n-1 degrees of freedom (von Storch and Zwiers 1999). The spread among individual ensemble members is given the 2.5th–97.5th percentile of trends; this reflects the range due to internal variability, and also inter-model uncertainty for the multi-model ensembles.

3. Reanalyses

We begin by considering recent trends in the annual-mean winds, as these are likely the most relevant for driving changes in the oceans. We find good agreement among the meteorological reanalyses, see **Figure 1**. All reanalyses show an increase in the strength of the zonal-mean and in the basin-average jets, with the increase in the Pacific jet (linear trend of 0.3-0.45 m/s per decade across the reanalyses) being considerably larger than the increase of the Atlantic-Indian jet (0.1-0.2 m/s per decade), see **Fig 1a-c**. Perhaps more striking, the Pacific jet has shifted *equatorward* (0.1-0.25^o per decade) whereas the Atlantic-Indian jet has shifted poleward (-0.25 to -0.4^o per decade), see **Fig 1e, f**. In other words, the Pacific and Atlantic-Indian jets have moved in opposite directions over the last 40 years. Note that although the equatorward shift in the Pacific jet is statistically insignificant at the 95% confidence level, the poleward shift of the Atlantic-Indian jet and the linear trend in latitudinal difference between the Pacific and Atlantic-Indian jets (0.4-0.5^o per decade) are statistically significant.

The different annual-mean trends between the Pacific and Atlantic-Indian jets are related to zonal asymmetries in *both* the climatological jet latitude and the wind trends. The climatological latitude of the annual-mean Pacific jet is poleward of the Atlantic-Indian jet (thick contour and horizontal lines in **Figure 2a**). At the same time the largest increase in winds occurs over the Pacific Ocean, and is equatorward of the regions of weak increases of the Atlantic and Indian oceans (**Figure 2a**). These larger trends over the Pacific than the other ocean basins are also found in satellite-based 10m winds, see figure 12 of Swart et al. (2015). As a result of these zonal variations, the largest zonal wind increase is equatorward of the jet over the Pacific sector (red curve in **Fig 2b**), yielding an equatorward shift of the Pacific jet shown in **Fig 1e**. In contrast there is an increase in winds poleward of the Atlantic-Indian jet (blue curve in **Fig 2b**), resulting in the poleward shift of the Atlantic-Indian jet (**Fig 1f)**.

The annual-mean strengthening of the jet shown in **Fig 1** comes mainly from strengthening in December-February (DJF) and March-May (MAM) (**Figs 2c-f, 3a**). However, there is strengthening all seasons (except for the Atlantic-Indian jet in September-November (SON)), and for all seasons the acceleration of the Pacific jet is stronger than that of the Atlantic-Indian jet (**Fig 3a**).

There is considerably more seasonality in zonal asymmetries in the trends in the jet latitude (see **Fig 3b**). The seasonality is largest over the Pacific: During DJF the largest wind increase in the Pacific is poleward of the jet, in MAM it is around the jet latitude, while in June-August (JJA) and SON the largest increase is equatorward of jet (**Fig 2**). This results in a poleward shift of the Pacific jet in DJF, an equatorward shift in SON, and weak movement in other seasons (**Fig 3b**). Thus, the annual-mean equatorward shift of the Pacific jet is the residual between a spring equatorward shift and summer poleward shift. The seasonality is much smaller for the Atlantic-Indian jet, with a poleward shift found in all seasons (**Fig 3b**). Note that while the direction of Pacific jet shift differs seasonally, for all seasons, the reanalysis-mean Pacific jet shifts equatorward relative to the Atlantic-Indian jet.

4. Climate Models

Several important questions arise from the above results. What are the causes of the observed trends and their zonal asymmetries? Are they a response to external forcing or merely internal variability? If the trends are forced, what is the forcing? If internal variability, is this driven by SSTs or is it internal to the atmosphere? Answering these questions is critical for understanding how the SH climate might evolve in the future.

To answer these questions, we analyze simulations from the CMIP5 and CanESM2 ensembles. Before addressing the issue of causality, we first determine whether the simulated and observed trends are consistent. Following Swart et al. (2005), we do this by determining whether the reanalysis trend falls within the 5^{th} – 95^{th} percentile of the simulated trends. For both the CMIP5 and CanESM2 historical simulations, the reanalysis trends for basin-averaged winds fall within (or very close to) the model spread across all seasons for both the strength and the latitude of the jet, see **Fig 4**. (Note, in Fig 4 the trends for the models and reanalyses are calculated for 1980-2005, the common period between reanalyses and CMIP5 historical runs.) Thus, these climate models can simulate trends similar to those observed.

We now consider the cause of these trends. Extensive previous research has shown that stratospheric ozone depletion and increasing GHGs have played a major role in the intensification and poleward shift of the zonal-mean jet in DJF (e.g., Polvani et al. 2011, McLandress et al. 2011, Banerjee et al. 2020). The CMIP5 and CanESM2 ensembles indicate this also applies for basin-averaged zonal winds. For both ensembles, models simulate a statistically significant ensemble-mean intensification and a poleward shift of the Pacific and Atlantic-Indian jets, with the vast majority of the simulations showing this intensification and poleward shift (**Fig. 4**). This consistency in sign among simulations indicates that forcing has played a major contribution to DJF trends in basin-average winds.

The central role of ozone depletion and increases in GHGs in the DJF trends is further supported by analysis of the CanESM2 "single forcing" ensembles (Supplementary Figure 1): For all basins, there are near-zero (insignificant) ensemble-mean shifts in the NAT and AA simulations (e.g. for Pacific jet the shift is 0.07± 0.1 and -0.02±0.1 degrees/decade for the NAT and AA, respectively), which indicates that changes in solar forcing, volcanic eruptions, and anthropogenic aerosols are not the cause. However, there are significant ensemble-mean DJF trends for the OZ forcing ensemble (-0.23±0.2 degrees/decade), and for the greenhouse gas forcing estimated as residual between the historical and the sum of the single-forcing runs (-0.33±0.3 degrees/decade). Therefore, DJF trends in jet latitude in the CanESM2 historical ensemble occur because of changes in stratospheric ozone and greenhouse gases.

We now consider the spring (SON) trends. Less attention has been paid to trends in this season but, as shown above, the equatorward shift of the Pacific jet during this season dominates the annual-mean change. For both the CMIP5 and CanESM2 historical ensembles the ensemble-mean Pacific and Atlantic-Indian jets strengthen and shift poleward, although these ensemble-mean trends are not always statistically significant (**Fig 4b**). The sign of the ensemble-mean trends for the Atlantic-Indian jet agrees with the reanalyses, but this is not the case for the Pacific jet, for which the reanalyses show a weakening and equatorward shift over the 1980-2005 period. However, for both metrics the spread in trends among the ensemble members is very large, and the observed trends lie within this spread. This suggests that the observed trends are not a forced response but result from internal variability. This interpretation is further supported by the CanESM2 single-forcing ensembles (Supplementary Figure 1): For each single-forcing ensemble we find a similar large spread in shift in the SON Pacific jet winds across the 50 members and an insignificant ensemble-mean shift in the Pacific jet in SON (0.18± 0.2, 0.19±0.2, -0.15±0.3 degrees/decade for the NAT, AA, and OZ ensembles, respectively)

The absence of a forced spring shift over the Pacific is supported by simulations that consider large increases in CO_2. Analysis of the CMIP5 4xCO_2 simulations shows a significant

ensemble-mean poleward shift in the jet for all basins in DJF, but for SON the shift in the Pacific jet is not significant, see **Fig 4b**. In SON (and JJA) there is again a large spread amongst models, and half of the models show an equatorward movement. In other words, the shift in peak JJA and SON Pacific jet due to quadrupling of CO_2 is much less than inter-model variability, indicating that increases in CO_2 are unlikely to have caused the observed historical equatorward shift. There is, however, a significant jet strengthening in all seasons in the 4xCO_2 simulations (**Fig 4a**, Supplementary Figure 2). Thus, while increases in CO_2 over the rest of this century are unlikely to force a significant movement in SON Pacific jet, the simulations analyzed here suggest that it might lead to an overall strengthening of this jet.

Finally, we examine the question of whether the winter-spring trends, which we interpret as internal variability, are coupled to ocean variability. To address this, we compare the ensemble of CMIP5 historical simulations with the ensemble of CMIP5 AMIP simulations. Although all the CMIP5 AMIP simulations use the same observationally-based SSTs, the spread in the jet shift is comparable to, if not larger than, the historical simulations and AMIP simulations, see **Fig 4b**, Supplementary Figure 2). Thus, internal atmospheric dynamics can generate large summer-spring trends in latitude of Pacific jet comparable to (and larger than) the observed trends. This conclusion that internal atmospheric variability plays an important role in multi-decadal trends in peak winds is consistent with the Garfinkel et al. (2015) analysis of trends in the width of the Hadley Cell.

5. Conclusions

Examination of meteorological reanalyses reveals substantial longitudinal variations in recent (post 1979) trends in SH near-surface winds, including variations in the strength and latitude of the jet. In the annual mean, the maximum winds strengthen in all basins, but the increase is larger over the Pacific than over the Indian and Atlantic Oceans. Furthermore, and perhaps more surprisingly, the meridional shift of the jet has been of opposite sign in different basins, with an equatorward shift over the Pacific but a poleward shift over the Indian and Atlantic Oceans. The annual-mean equatorward shift in the Pacific jet is caused by a spring equatorward shift that is much larger than the summer-fall poleward shift.

As shown in previous studies, we find that stratospheric ozone depletion and increasing GHGs have played a major role in the strengthening and poleward shift of the DJF jet, for the zonal-mean as well as for the basin-averages. However, the simulations analyzed here indicate that winter-spring trends in the Pacific jet latitude are not a forced response but are due to very large internal variability. Furthermore, comparison of coupled and atmosphere-only simulations suggest this shift is due to internal atmospheric variability, rather than coupled atmosphere-ocean variability. The lack of a forced winter-spring shift in the Pacific jet extends to a quadrupling of CO_2. We have found a significant ensemble-mean poleward shift in the Pacific jet in DJF and MAM for 4xCO_2 simulations, but not in JJA or SON. This suggest that increases in CO_2 - and other GHGs - over the rest of this century are also unlikely to force a significant movement of winter-spring peak winds over the Pacific.

Much of the research on trends in SH atmosphere and ocean circulation has emphasized the poleward shift of the westerlies. However, as shown here, over the Pacific sector, in winter and spring (and in the annual-mean) the westerlies have actually shifted equatorward. This equatorward shift will likely lead to opposite changes in storm tracks and precipitation, as well as in the ocean circulation, over the Pacific sector compared to other sectors. While these zonal

differences in trends may only apply to winter-spring, the shift in annual-mean winds – and the longer response time of the oceans to wind forcing -– may result in more persistent zonal asymmetries in ocean trends. For example, as the ocean gyre circulation responds to changes in basin-wide wind stresses, the opposite trends in Pacific and Atlantic-Indian jets suggest that trends in respective gyres may have also been of opposite sign. This then may result in zonal asymmetries in ocean ventilation, heat and carbon uptake, and sea level changes (e.g., Zhang et al. 2014, Jones et al. 2019, Waugh et al. 2019, Keppler and Landschützer 2019).

Acknowledgments

The reanalysis datasets can be downloaded from their respective webservers: The European Centre for Medium-Range Weather Forecasts (ECMWF) for ERA-I (https://apps.ecmwf.int/datasets/data/interim-full-daily/levtype=sfc/), the JMA Data Dissemination System (JDDS) for JRA-55 (https://jra.kishou.go.jp/JRA-55/index_en.html#download) and the Goddard Earth Sciences Data and Information Services Center (GES DIC) for MERRA2 (https://disc.gsfc.nasa.gov/datasets?keywords=%22MERRA-2%22&page=1&source=Models%2FAnalyses%20MERRA-2). The model output for CanESM2 can be accessed at: http://climate-modelling.canada.ca/climatemodeldata/cgcm4/CanESM2/index.shtml, while the CMIP5data used in this study are freely available through the Earth System Grid Federation (https:// esgf-node.llnl.gov). We acknowledge the World Climate Research Programme's Working Group on Coupled Modelling, which is responsible for CMIP, and we thank the climate modeling groups for producing and making available their model output. We also acknowledge the Environment and Climate Change Canada's Canadian Centre for Climate Modelling and Analysis for executing and making available the CanESM2 Large Ensemble simulations used in this study. DWW and LMP are supported by grants from the US National Science Foundation to Columbia University.

References

Banerjee A, Fyfe, J.C., Polvani, L. M., and Waugh, D.W. (2020), A pause in Southern Hemisphere circulation trends due to the Montreal Protocol, *Nature,* 579: 544–548

Cai W, Cowan T, Godfrey S, Wijffels S (2010), Simulation of processes associated with the fast warming rate of the southern midlatitude ocean. *J Climate*, 23:197–206

Dee, D. P. et al. (2011), The ERA-Interim reanalysis: configuration and performance of the data assimilation system. *Q. J. R. Meteorol. Soc.,* 137, 553–597.

Gagné, M.-È., J. C. Fyfe, N. P. Gillett, I. V. Polyakov, and G. M. Flato, 2017: Aerosol-driven increase in Arctic sea ice over the middle of the twentieth century, *Geophys. Res. Lett.,* 44, 7338–7346.

Garfinkel, C. I., D. W. Waugh, and L. M. Polvani (2015), Recent Hadley cell expansion: the role of internal atmospheric variability in reconciling modeled and observed trends. *Geophys. Res. Lett.*, 42, 10824–10831,

Gelaro, R. et al. (2017), The Modern-Era Retrospective Analysis for Research and Applications, Version 2 (MERRA-2). *J. Climate*, 30, 5419–5454

Grise, K. M., and L. M. Polvani (2014), Is climate sensitivity related to dynamical sensitivity? A Southern Hemisphere perspective. *Geophys. Res. Lett.,* 41, 534–540.

Grise, K. M., and L. M. Polvani (2016), Is climate sensitivity related to dynamical sensitivity? *J. Geophys. Res. Atmos.*, 121, 5159–5176

Grise, K. M. et al. (2019), Recent tropical expansion: natural variability or forced response? *J. Climate,* 32, 1551–1571.

Hall, A. and Visbeck, M., (2002), Synchronous variability in the Southern Hemisphere atmosphere, sea ice, and ocean resulting from the annular mode. *Journal of Climate*, *15*(21), pp.3043-3057.

Hendon, H.H., Thompson, D.W. and Wheeler, M.C., (2007), Australian rainfall and surface temperature variations associated with the Southern Hemisphere annular mode. *Journal of Climate*, *20*(11), pp.2452-2467.

Jones, D. C., Boland, E. J., Meijers, A. J. S., Forget, G., Josey, S. A., Sallee, J.-B., and Shuckburgh, E. (2019). Heat distribution in the Southeast Pacific is only weakly sensitive to high-latitude heat flux and wind stress. *Journal of Geophysical Research: Oceans*, 124, 8647– 8666.

Keppler, L., & Landschützer, P. (2019). Regional wind variability modulates the Southern Ocean carbon sink. *Scientific reports*, *9*(1), 1-10.

Kobayashi, S. et al. (2015), The JRA-55 Reanalysis: general specifications and basic characteristics. *J. Meteorol. Soc. Jpn*., 93, 5–48.

Le Quere, C., Rödenbeck, C., Buitenhuis, E.T., Conway, T.J., Langenfelds, R., Gomez, A., Labuschagne, C.Ramonet, M., Nakazawa, T., Metzl, N. & Gillett, N. (2007), Saturation of the Southern Ocean CO2 sink due to recent climate change. *Science*, 316, 1735-1738

McLandress, C., T. G. Shepherd, J. F. Scinocca, D. A. Plummer, M. Sigmond, A. I. Jonsson, and M. C. Reader (2011), Separating the dynamical effects of climate change and ozone depletion. Part II: Southern Hemisphere troposphere, *J. Clim.*, *24*(6), 1850–1868.

Polvani, L. M., D. W. Waugh, G. J. P. Correa, and S.-W. Son (2011), Stratospheric ozone depletion: The main driver of twentieth-century atmospheric circulation changes in the Southern Hemisphere, *J. Climate*, *24*, 795–812.

Roemmich, D., J Gilson, R. Davis, P. Sutton, S. Wijffels, & S. Riser, (2007), Decadal Spinup of the South Pacific Subtropical Gyre, *J. Phys. Ocean*., 37, 162

Schneider, D. P., Deser, C. and Fan T. (2015), Comparing the Impacts of Tropical SST Variability and Polar Stratospheric Ozone Loss on the Southern Ocean Westerly Winds, *Journal of Climate*, 28, 9350-9372.

Sen Gupta, A. and England, M.H., 2006. Coupled ocean–atmosphere–ice response to variations in the southern annular mode. *Journal of Climate*, *19*, 4457-4486.

Swart, N.C. & J.C. Fyfe, 2012: Observed and simulated changes in the Southern Hemisphere surface westerly wind-stress, *Geophys. Res. Lett.,* 39, L16711, doi:10.1029/2012GL052810

Swart, N. C., Fyfe, J. C., Gillett, N. & Marshall, G. J. (2015), Comparing trends in the Southern Annular Mode and surface westerly jet. *J. Climate*, 28, 8840–8859.

Taylor, K.E., R.J. Stouffer, and G.A. Meehl (2012), An overview of CMIP5 and the experiment design. *Bull. Amer. Meteor. Soc.,* 93, 485–498.

Thompson DWJ, Solomon S, Kushner PJ, England MH, Grise KM, Karoly DJ. (2011), Signatures of the Antarctic ozone hole in Southern Hemisphere surface climate change. *Nat. Geosci.* 4, 471–479

Toggweiler, J.R. and Russell, J., (2008), Ocean circulation in a warming climate. *Nature*, *451*, 286-288

Thompson, D. W. J., and J. M. Wallace (2000), Annular modes in the extratropical circulation: I. Month-to-month variability, *J. Climate*, 13, 1000 – 1016.

Thompson, D. W., Solomon, S., Kushner, P. J., England, M. H., Grise, K. M., & Karoly, D. J. (2011). Signatures of the Antarctic ozone hole in Southern Hemisphere surface climate change. *Nature Geoscience*, *4*(11), 741-749.

Waugh, D. W. et al. (2018), Revisiting the relationship among metrics of tropical expansion. *J. Climate*. 31, 7565–7581.

Waugh, D. W., F. Primeau, T. DeVries, and M. Holzer (2013), Recent changes in the ventilation of the southern oceans, *Science*, 339, 568.

Yang, D., Arblaster, J. M., Meehl, G. A., England, M. H., Lim, E. P., Bates, S., & Rosenbloom, N. (2020). Role of tropical variability in driving decadal shifts in the Southern Hemisphere summertime eddy-driven jet. *Journal of Climate*, https://doi.org/10.1175/JCLI-D-19-0604.1

Zhang, X., Church, J.A., Platten, S.M. and D Monselesan (2014), Projection of subtropical gyre circulation and associated sea level changes in the Pacific based on CMIP3 climate models. *Climate dynamics*, *43*, 131-144

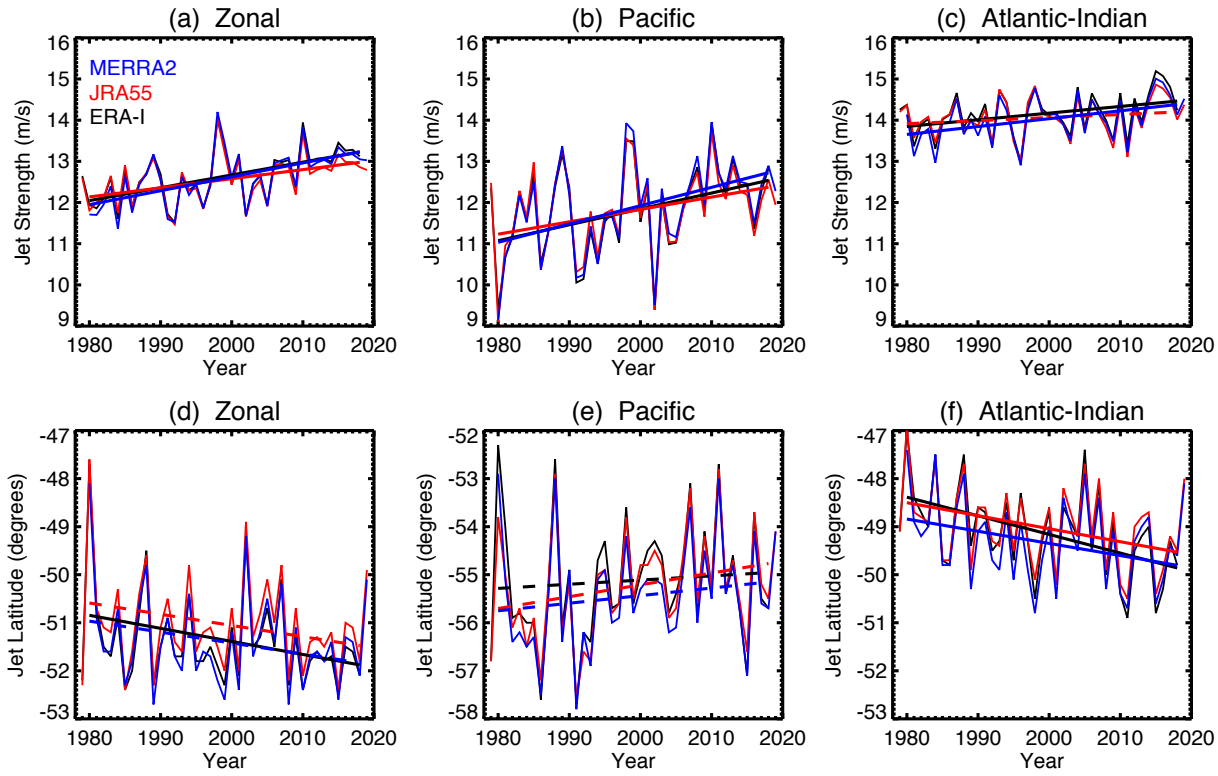

Figure 1: Time series of jet (a-c) strength and (d-f) position, for (a,d) zonal-mean, (b,e) Pacific, and (c,f) Atlantic-Indian averages. Different colors for MERRA2, JRA55, and ERA-I reanalyses, with lines show 1980-2018 linear trends (solid if significant at 95% confidence level). Note, y-axis for Pacific latitude is shifted relative to the zonal-mean and Atlantic-Indian mean.

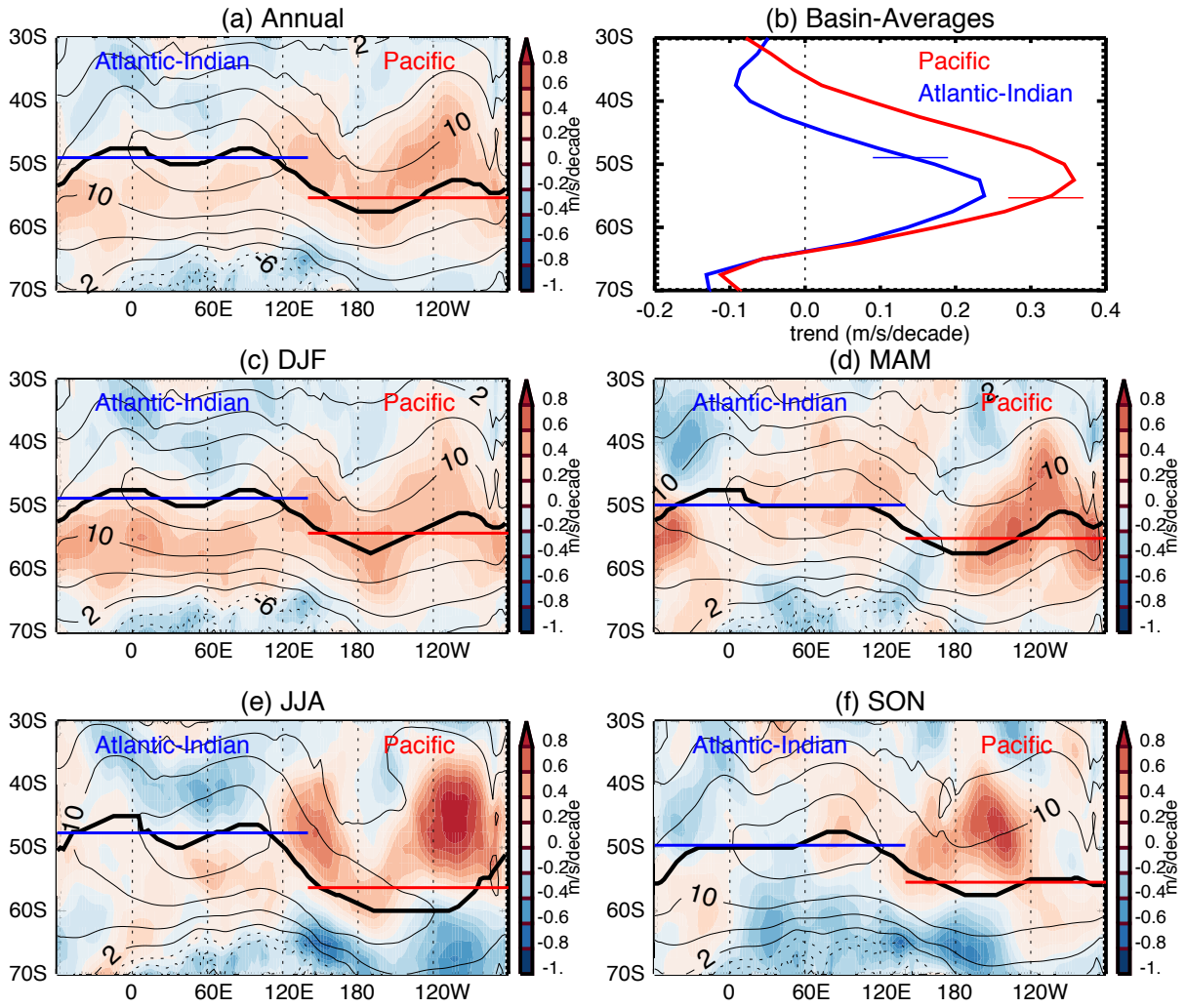

Figure 2: Maps of trends (colors) and climatology (contours) of 850 hPa zonal winds for 1980-2018 for (a) annual-mean, (c) DJF, (d) MAM, (e) JJA and (f) SON, and (b) variations of trends in basin-average winds with latitude. Contours in panels (a), (c)-(f) show climatological winds (interval of 2 m/s), thick curve shows climatological location of jet at each longitude, and horizontal lines show climatological-mean location of the Atlantic-Indian and Pacific jets. In panel (b) the horizontal bars show the climatological-mean location of the Atlantic-Indian and Pacific jets. All fields are based on the winds averaged over the three reanalyses.

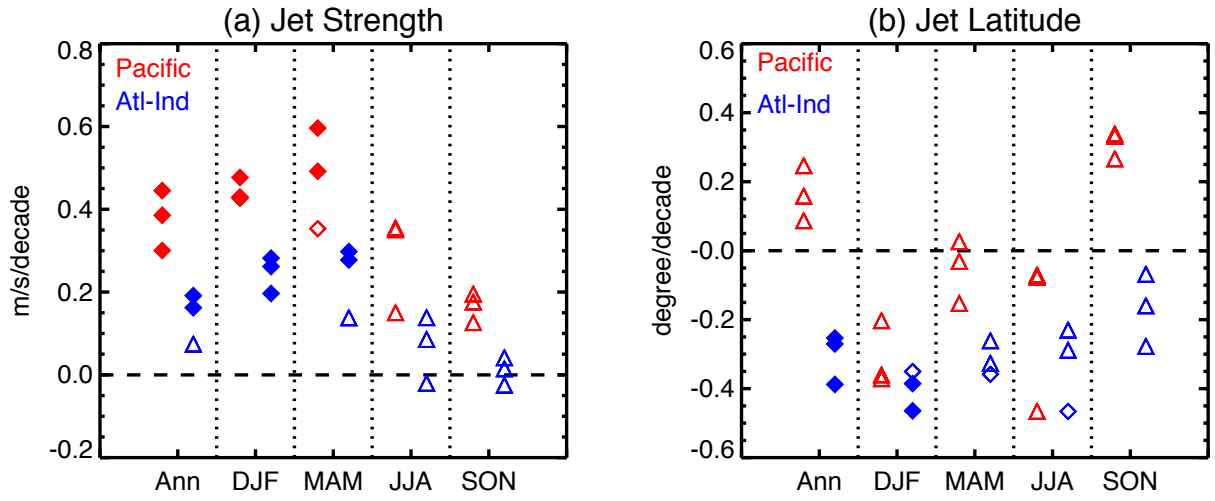

Figure 3: Seasonal variations in trends in (a) strength and (b) latitude for Pacific (red) and Atlantic-Indian (blue) jet. Separate symbols for each of ERA, JRA55, and MERRA-55, with filled diamond indicating statistical significance at 95%, open diamond significant at 90%, and triangle not significant at 90%.

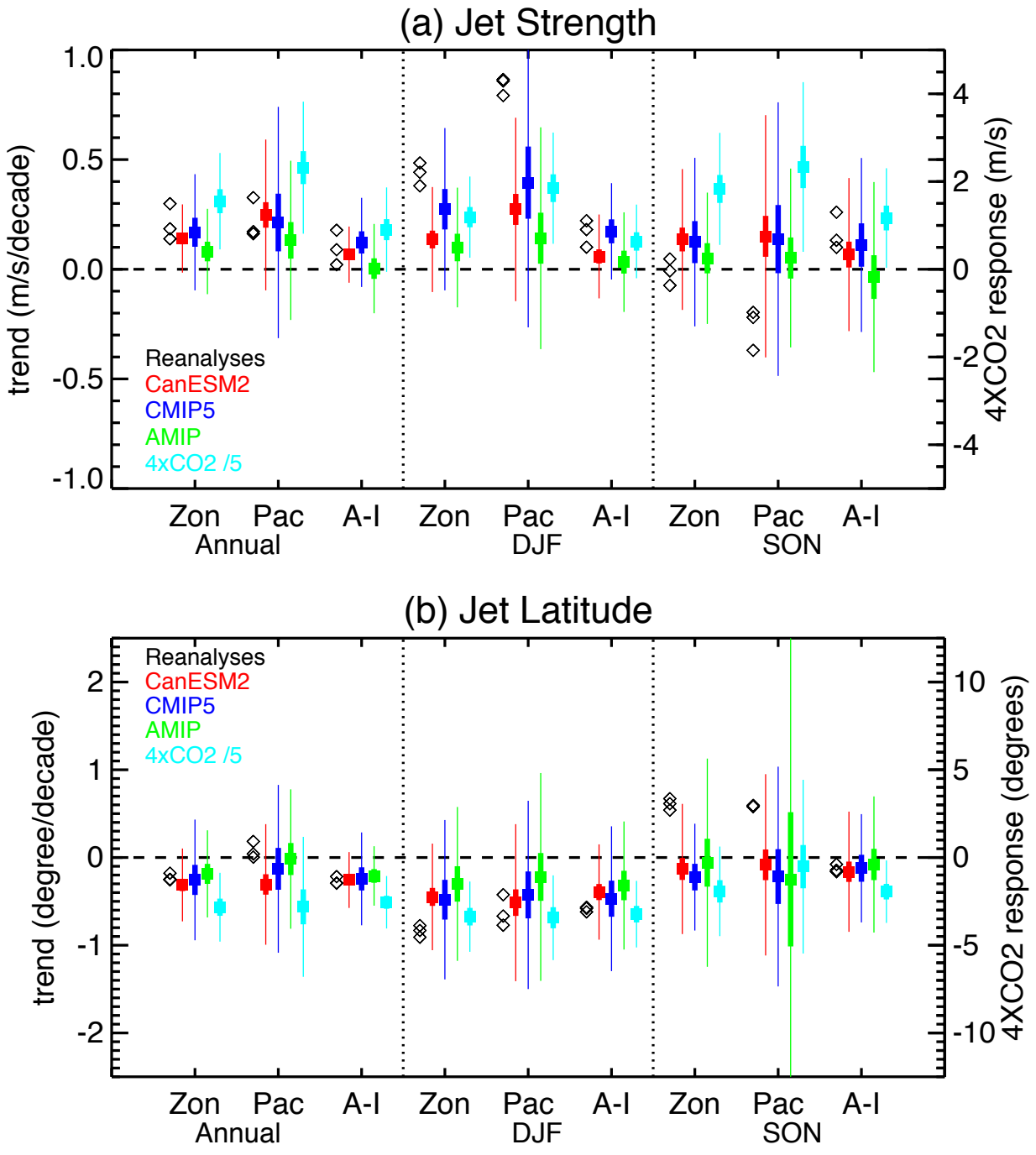

Figure 4: Trends in jet (a) strength and (b) latitude for reanalyses (black), CanESM2 historical (red), CMIP5 historical (blue), CMIP5 AMIP (green), and CMIP5 4xCO2 (cyan) ensembles. Trends are for 1980-2005 in reanalyses and models, except for 4xCO2 where difference between end of 4xCO2 simulations and PI simulation are shown (right axes). For the models the square shows the ensemble mean, thick vertical bar the 95% confidence interval on this mean, and thin bar the 2.5th–97.5th percentiles of the trends.

Model Name
ACCESS1-0
bcc-csm1-1
bcc-csm1-1-m
CanESM2
CCSM4
CNRM-CM5
CSIRO-Mk3-6-0
FGOALS-s2
GFDL-CM3
GISS-E2-R
HadGEM2-ES
inmcm4
IPSL-CM5A-LR
IPSL-CM5B-LR
MIROC5
MIROC-ESM
MPI-ESM-LR
MPI-ESM-MR
MRI-CGCM3
NorESM1-M

Supplementary Table 1: CMIP5 models used in the analysis.

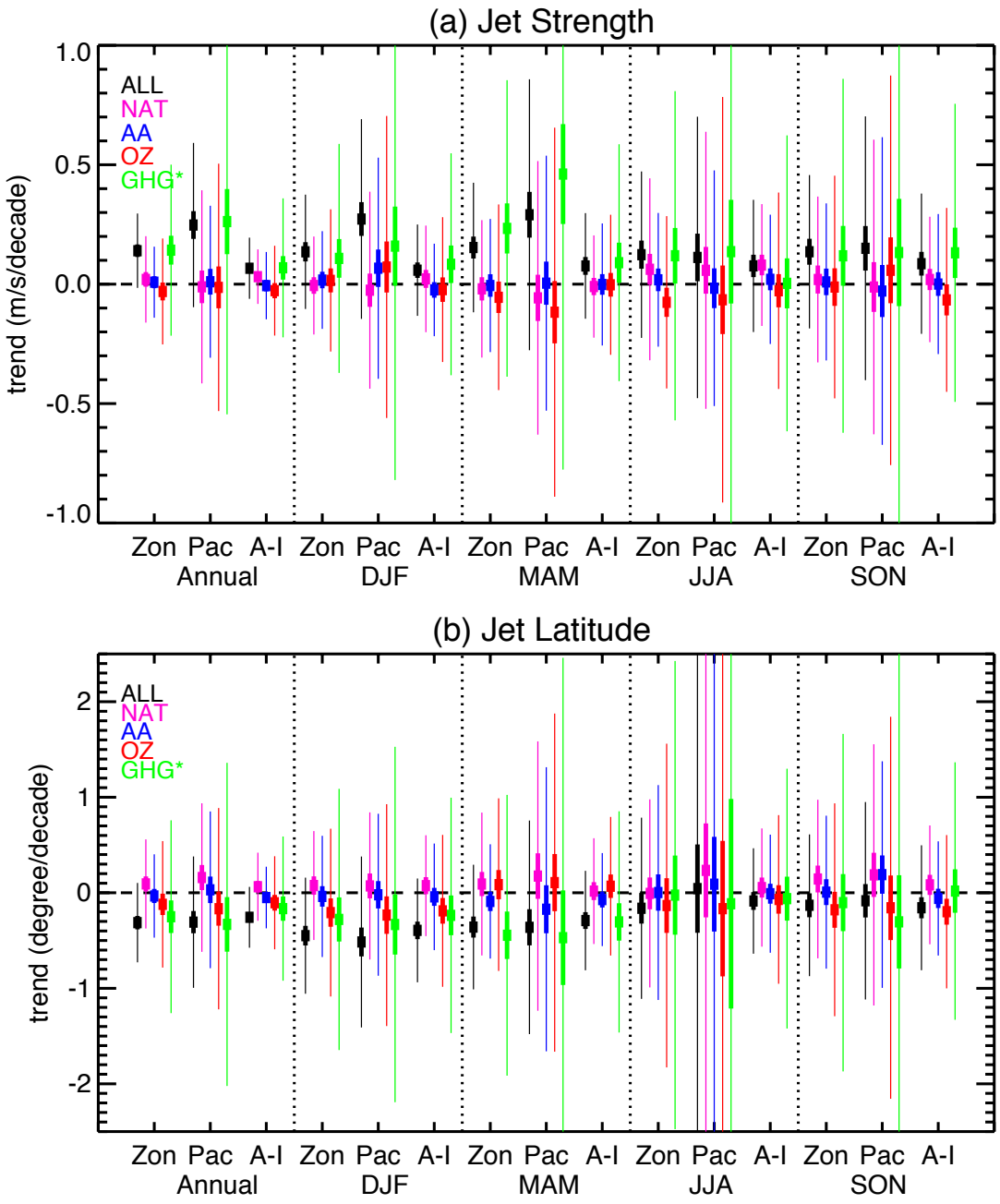

Supplementary Figure 1: As in Figure 4 except for trends in jet (a) strength and (b) latitude for different CanESM2 ensembles, for all seasons.

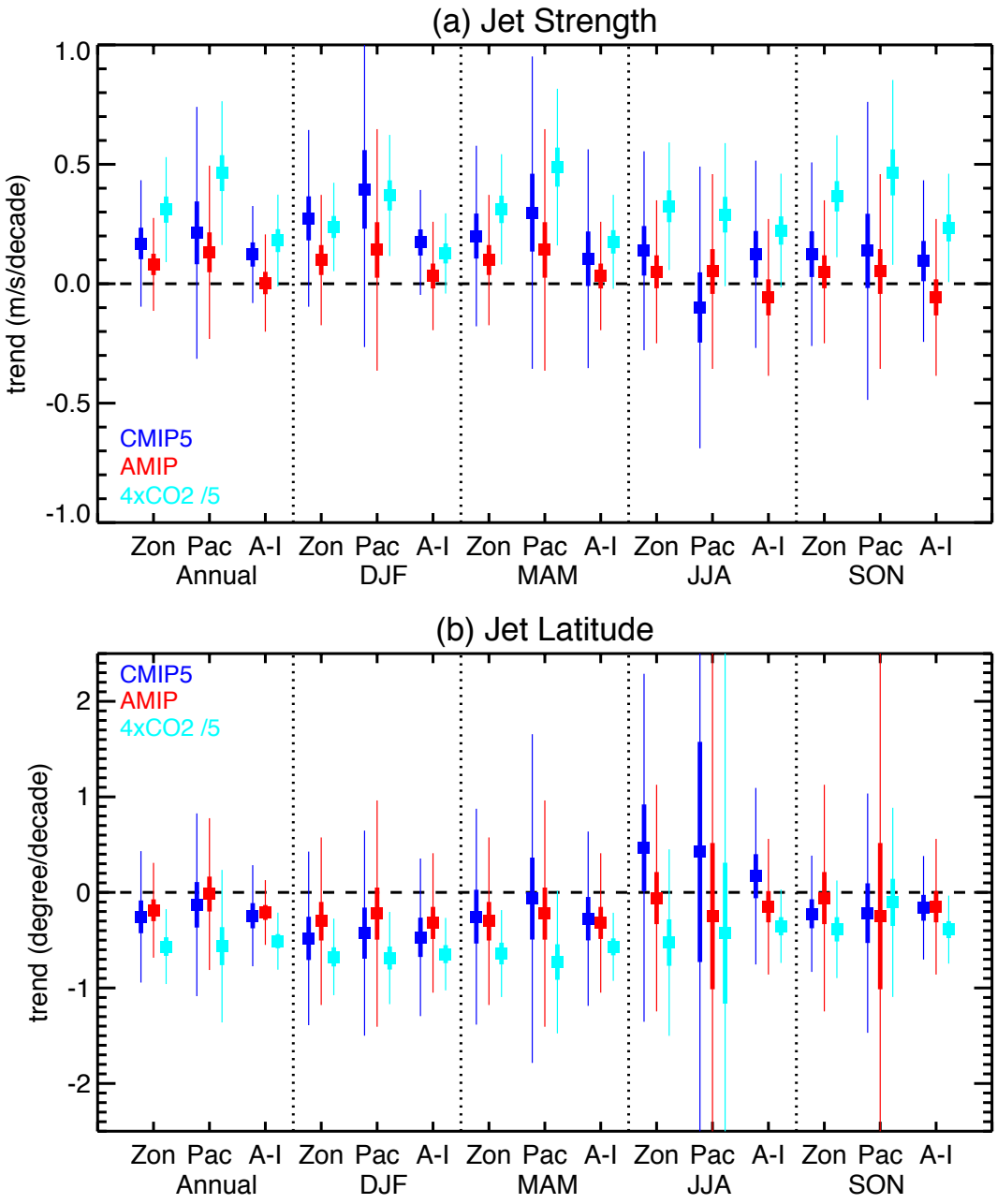

Supplementary Figure 2: As in Figure 4 except for trends in jet (a) strength and (b) latitude for CMIP5 historical, AMIP, and 4xCO2 ensembles, for all seasons.